



OPEN

Green phosphorescent organic light-emitting diode exhibiting highest external quantum efficiency with ultra-thin undoped emission layer

Shin Woo Kang^{1,2}, Dong-Hyun Baek³, Byeong-Kwon Ju^{1✉} & Young Wook Park^{2✉}

In this study, we report highly efficient green phosphorescent organic light-emitting diodes (OLEDs) with ultra-thin emission layers (EMLs). We use tris[2-phenylpyridinato-C₂N]iridium(III) (Ir(ppy)₃), a green phosphorescent dopant, for creating the OLEDs. Under systematic analysis, the peak external quantum efficiency (EQE) of an optimized device based on the ultra-thin EML structure is found to be approximately 24%. This result is highest EQE among ultra-thin EML OLEDs and comparable to the highest efficiency achieved by OLEDs using Ir(ppy)₃ that are fabricated via conventional doping methods. Moreover, this result shows that OLEDs with ultra-thin EML structures can achieve ultra-high efficiency.

Research has been progressing on organic light-emitting diodes (OLEDs), ever since they were first developed in 1987 by Tang et al.¹. From then, to the present, OLEDs have attracted remarkable amounts of attention and undergone much development, because of several advantages such as their lightweight, thin, flexible, and stretchable structures, and variable form factors^{2–5}. Owing to these advantages, OLEDs are currently attracting much attention in the television, monitor, mobile, and other display markets. However, certain problems remain to be solved. For instance, the devices exhibit problems in terms of their efficiency, lifetime, etc.; their fabrication involves problems related to the long processing time, complicated processes, requirement of high-level vacuum, etc.^{6,7}. Much research is being conducted to solve these problems. To increase the efficiency of the OLEDs, the development of organic materials, optimization of the device structure, and improvement of the outcoupling efficiency are necessary. The development of organic materials began with fluorescent materials and proceeded to phosphorescent and thermally activated delayed fluorescent (TADF) materials^{8,9}. The maximum achievable internal quantum efficiency (IQE) was 25% for fluorescent devices emitting only a singlet exciton state^{10,11}. Phosphorescent devices and TADF devices that utilized triplets for light emission through intersystem crossing (ISC) or reverse intersystem crossing (RISC) could achieve IQEs up to 100%^{4,6,10–12}. The triplet excitons of phosphorescent devices had high probabilities of dissociation by meeting each other, because of the long lifetime. The high density of triplet excitons caused triplet–triplet annihilation (TTA) and triplet–polaron quenching (TPQ)^{13–16}. In order to prevent TTA and achieve high efficiency, an appropriate doping concentration is required. In a doping method conventionally used in low-molecular OLEDs, a host and dopant were simultaneously deposited on an emission layer (EML) in a specific ratio, which was determined by the weight percent. In other words, the deposition rates of the host and dopant were determined by the doping ratio, which was a difficult process requiring very precise control of the deposition rate and deposition thickness monitoring. Because of this difficulty with regard to doping, research has been conducted to fabricate OLEDs without the use of conventional doping methods^{17–20}. Although Xu et al. reported 38% EQE with ultra-thin EML, however, it was used tandem structure. Theoretically, the tandem structure is formed by several single units, the EQE and current efficiency

¹Display and Nanosystem Laboratory, School of Electrical Engineering, Korea University, 145, Anam-ro, Seongbuk-gu, Seoul 02841, Republic of Korea. ²Nano and Organic-Electronics Laboratory, Department of Display and Semiconductor Engineering, Sun Moon University, Asan, Chungcheongnam-do 31460, Republic of Korea. ³Center for Next Generation Semiconductor Technology, Department of Display and Semiconductor Engineering, Sun Moon University, Asan, Chungcheongnam-do 31460, Republic of Korea. ✉email: bkju@korea.ac.kr; zerook@sunmoon.ac.kr

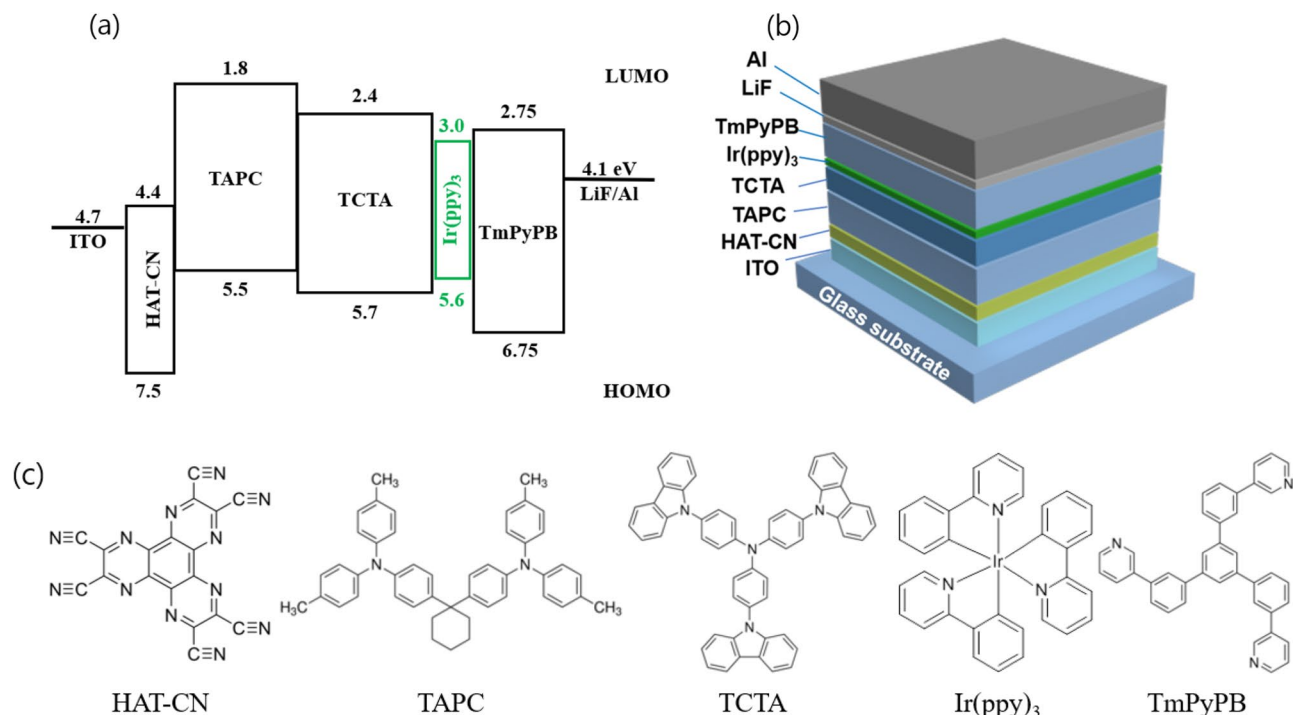


Figure 1. (a) Energy level diagram of OLED device with ultra-thin EML structure. (b) Fabricated OLED device structure. (c) Molecular structures of the organic materials used in the device.

of the tandem device increase by X times with the number of single units²⁰. Therefore, it should not merely accept the face value.

We fabricated OLEDs with ultra-thin EML structures using tris[2-phenylpyridinato-C2,N]iridium(III) (Ir(ppy)₃). The fabricated devices were optimized via precise control over the optical path length (OPL) and charge balance of the device structures, without the usage of any light extraction technology. The resulting external quantum efficiency (EQE) of 23.8% showed that OLEDs with ultra-thin EMLs could achieve comparably higher efficiencies than the OLEDs with conventionally doped EMLs. The demonstrated EQE (23.8%) was the highest among that of the devices that did not use tandem structure, novel hosts or transporting layers; it was also comparable to that of the device with the highest efficiency.

Results

In this study, OLEDs with ultra-thin EMLs were fabricated. The ultra-thin EML structure referred to a structure in which a dopant was inserted into the EML position—for example, between a the hole transport layer (HTL) and electron transport layer (ETL), with very small thickness in the order of several nanometres or less, without the use of a conventional doping method. Figure 1a shows the energy level diagram of the fabricated OLEDs with ultra-thin EML structures, and Fig. 1b shows a schematic of the fabricated OLEDs. Figure 1c shows the molecular structures of the organic materials used in this device.

First, OLEDs with the structure dipyrzino[2,3-f;2',3'-h]quinoxaline-2,3,6,7,10,11-hexacarbonitrile (HAT-CN) 0.5 nm/di-[4-(N,N-di-p-tolyl-amino)-phenyl]cyclohexane (TAPC) 85 nm/4,4',4''-Tris(carbazole-9-yl)triphenylamine (TCTA) 30 nm/Tris[2-phenylpyridinato-C2,N]iridium(III) (Ir(ppy)₃) X nm/1,3,5-Tri[(3-pyridyl)phen-3-yl]benzene (TmPyPB) 75 nm/lithium fluoride (LiF) 1 nm/aluminum (Al) were fabricated to determine the optimum thin-EML thickness by balancing the energy transfer and trapping emissions while minimizing the TTA. The dopant thickness of X nm was adjusted from 0.05 to 0.2 nm to determine the optimum dopant thickness at which the energy transfer from the adjacent layer and direct light emission by trapping of dopants occurred most efficiently. Figure 2 shows the peak EQE, according to the dopant thickness of the fabricated OLEDs; the inset shows the current–density–EQE characteristics according to the dopant thickness.

We can observe that the efficiency was the highest at the thickness of 0.075 nm. Between 0.05 and 0.10 nm, the peak EQE exhibited peaks, but reduced greatly at larger thicknesses. This suggests that thicknesses greater than 0.1 nm can result in exciton quenching such as TTA^{15,16}.

The Ir(ppy)₃ ultra-thin EML OLEDs were fabricated considering the optimum thickness of 0.075 nm, and were then optimized further. Multiple sets of devices with different thickness of the ultra-thin layer were compared while controlling the thicknesses of the other layers [including hole injection layer (HIL), HTL, ETL, and electron injection layer (EIL)] simultaneously. Among all such devices, the device with the 0.075-nm thick ultra-thin EML showed the highest efficiency, within the boundary of first-order constructive interference. This suggested that the thickness of 0.075 nm was finely optimized for high-efficiency ultra-thin Ir(ppy)₃ EML OLEDs.

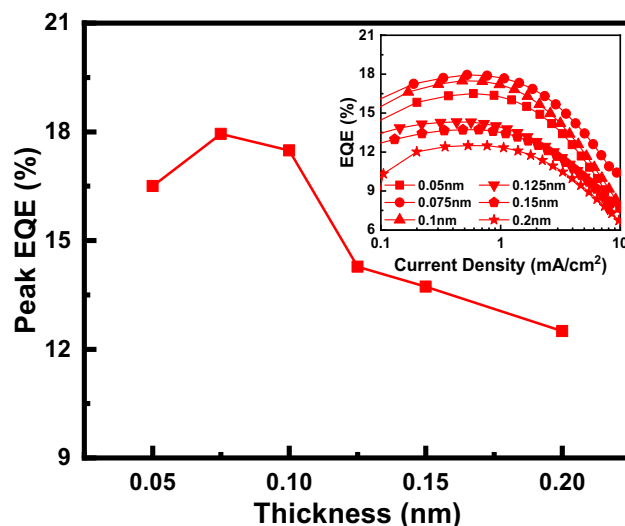


Figure 2. Peak EQE versus thickness of Ir(ppy)₃ from 0.05 to 0.2 nm. The inset shows the EQE characteristics of the fabricated OLEDs, as a function of current density.

To analyse the electroluminescence (EL) characteristics of OLEDs with ultra-thin EML in more depth, we compared the ultra-thin EML method and conventional doping method of OLEDs. In the two doping methods, the dopant molecules have different molecular distribution. The dopants of ultra-thin EML are distributed in a two-dimensional form (in-planar). However, the hosts and the dopants of conventional doping method are mixed in three-dimensional form. Due to this difference, direct comparison is difficult to conduct. Therefore, the ultra-thin EML method and the conventional doping method are indirectly compared and analysed using the intermolecular distance of dopant molecules, which is an important variable in the host-dopant energy transfer process. The average intermolecular distance of dopants was calculated by the assuming that the ultra-thin EML method and conventional doping method have a uniform molecular distribution in two and three dimensions, respectively [Supporting Information-1].

To compare the ultra-thin EML method and the conventional doping method, photoluminescence (PL) and EL quantum efficiency data were referred from in researches result of the CBP:Ir(ppy)₃ doping structure in the form of a solid-state thin film, and a widely used doping structured phosphorescent OLEDs, respectively^{21,22}. Figure 3 shows the relationship between the quantum efficiencies and the average intermolecular distance of dopant according to the dopant thickness in the ultra-thin EML method (this work) and the doping concentration in the conventional doping method (from references^{21,22}). As in Fig. 3a, the thickness of 0.075 nm ultra-thin EML, which showed the highest efficiency, was interpreted with average dopant intermolecular distance of 4.0 nm. As we mentioned with Fig. 2, the shorter intermolecular distance of 3.5 nm results the increased TTA and decreased efficiency (0.1 nm ultra-thin EML). These characteristics can be confirmed by the results of other researches (Fig. 3b,c). The maximum PL quantum efficiency of doped thin solid film was showed at the doping concentration of 1.5 mol% and the average dopant intermolecular distance of ~ 4.3 nm. While maximum EL quantum efficiency of phosphorescent OLEDs was showed at the doping concentration of 6 wt% and the average dopant intermolecular distance of ~ 3 nm. And they were decreased with the increased doping ratio and average dopant intermolecular distance. As a summary, the PL quantum efficiency of the thin film and the EQE of the phosphorescent OLEDs showed the high-maximum efficiency with an average dopant intermolecular distance of 3 nm or more, while the efficiency decreased rapidly with the average dopant intermolecular distance of below 3 nm. That is, as the average dopant intermolecular distance decreases, the density of the triplet increases. The increase of the triplet density causes TTA, which in turn leads to decrease efficiency. And these results shows good consistency with TTA theory of high exciton quenching with below 3 nm as in literatures¹⁶.

To maximize the efficiency, the injection layer was controlled carefully for improved carrier balance. The initial thickness of the HTL and ETL were calculated and fixed at 80 and 74 nm, respectively, which were calculated to have constructive internal interference OPLs [Supporting Information 2]. Figure 4 shows the normalized (by maximum peak efficiency) EQE characteristics, as a function of the current density. Figures 4a,b show the EL characteristics depending on the thickness of the injection layer, HAT-CN (0.25–1.0 nm) and LiF (0.5–1.5 nm), respectively.

A clear dependence on the injection layer thickness was observed. The 0.25-nm thick HAT-CN and 1.0-nm thick LiF showed the highest efficiencies. Between the HIL and EIL, the EIL showed a much larger dependence, which meant that this device structure was hole dominant and carrier unbalanced. This result also suggested that much enhancement could be achieved by optimizing the HTL and ETL thicknesses or by using a high-mobility ETL^{23,25}.

However, modifying the carrier balance by controlling the thickness of the transport layer could have a negative effect on the internal interference matching of the OPL. Therefore, we investigated the correlation between

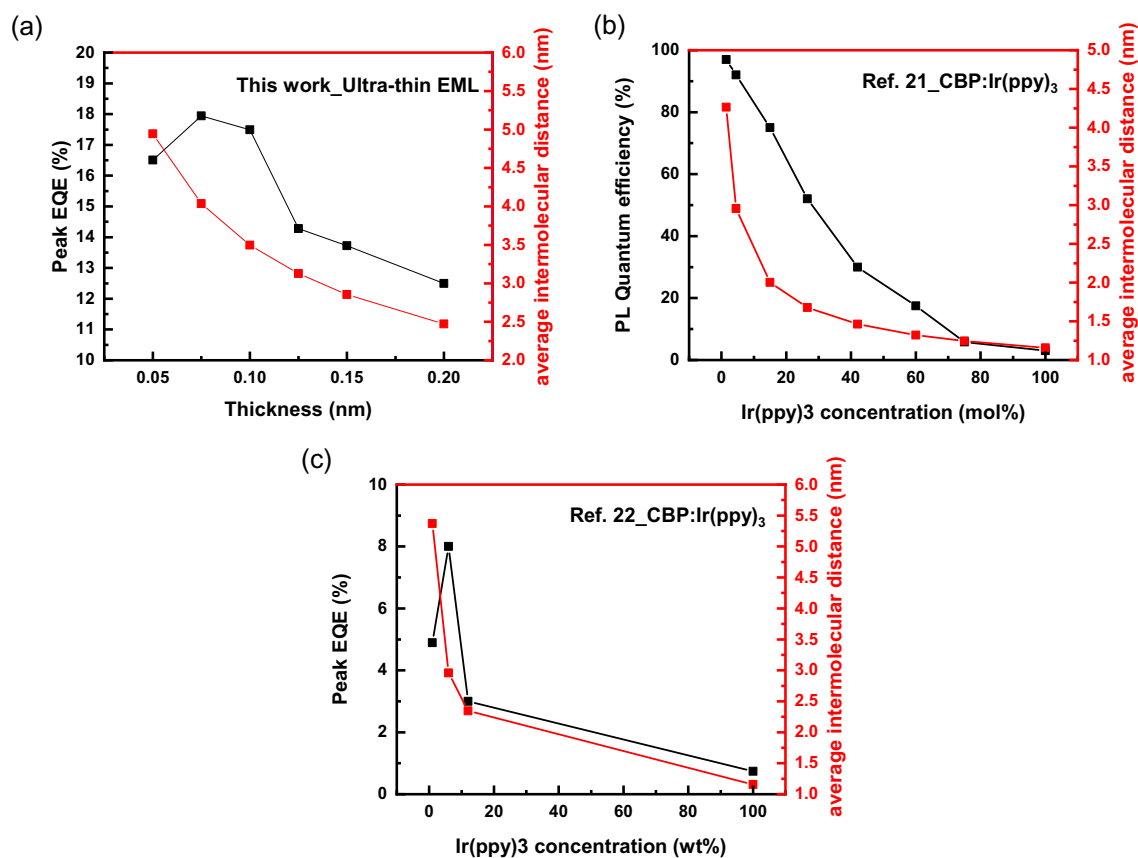


Figure 3. The relation between quantum efficiency and average dopant intermolecular distance according to the thickness of ultra-thin EML and doping concentration (a) this work, (b) reference²¹, and (c) reference²².

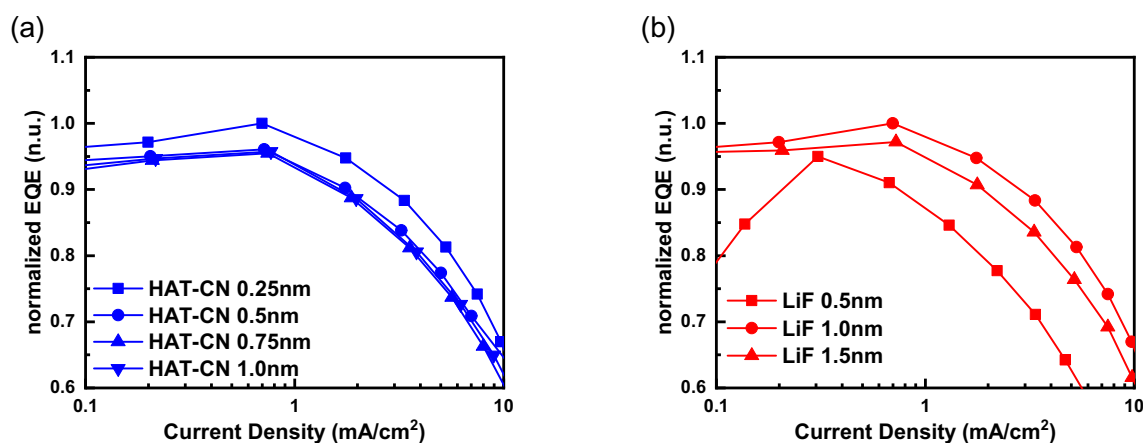


Figure 4. Normalized EQE characteristics as a function of current density: (a) HIL (HAT-CN) thickness changed, (b) EIL (LiF) thickness changed.

the optical efficiency (constructive interference) and carrier balance. The thicknesses of the dopant, HIL, and EIL were fixed at 0.075, 0.25, and 1.0 nm, respectively. The thicknesses of the HTL and ETL were step-wise varied from the calculated values; the HTL thickness was varied from 65 to 95 nm, and the ETL thickness from 54 to 104 nm. Figures 5a–c show the EL characteristics of six representative devices (HTL–ETL: 65–54, 80–54, 95–54, 80–74, 80–89, 80–104). Figure 5d shows a summary of the peak EQE data of all OLEDs. The detailed EL characteristics of the fabricated OLEDs are presented in the supporting information [Supporting Information-3].

In Fig. 5, among the HTL-controlled devices of different thicknesses, the 80-nm thick HTL showed the highest efficiency, as determined in Supporting Information—3. However, the effect of thickness of the ETL was different. On comparing the devices of 80–54, 80–74, 80–89, and 80–104, the EL efficiencies decreased following an increase in ETL thickness. This is verified by Fig. 5d, which presents the EQEs of all fabricated devices.

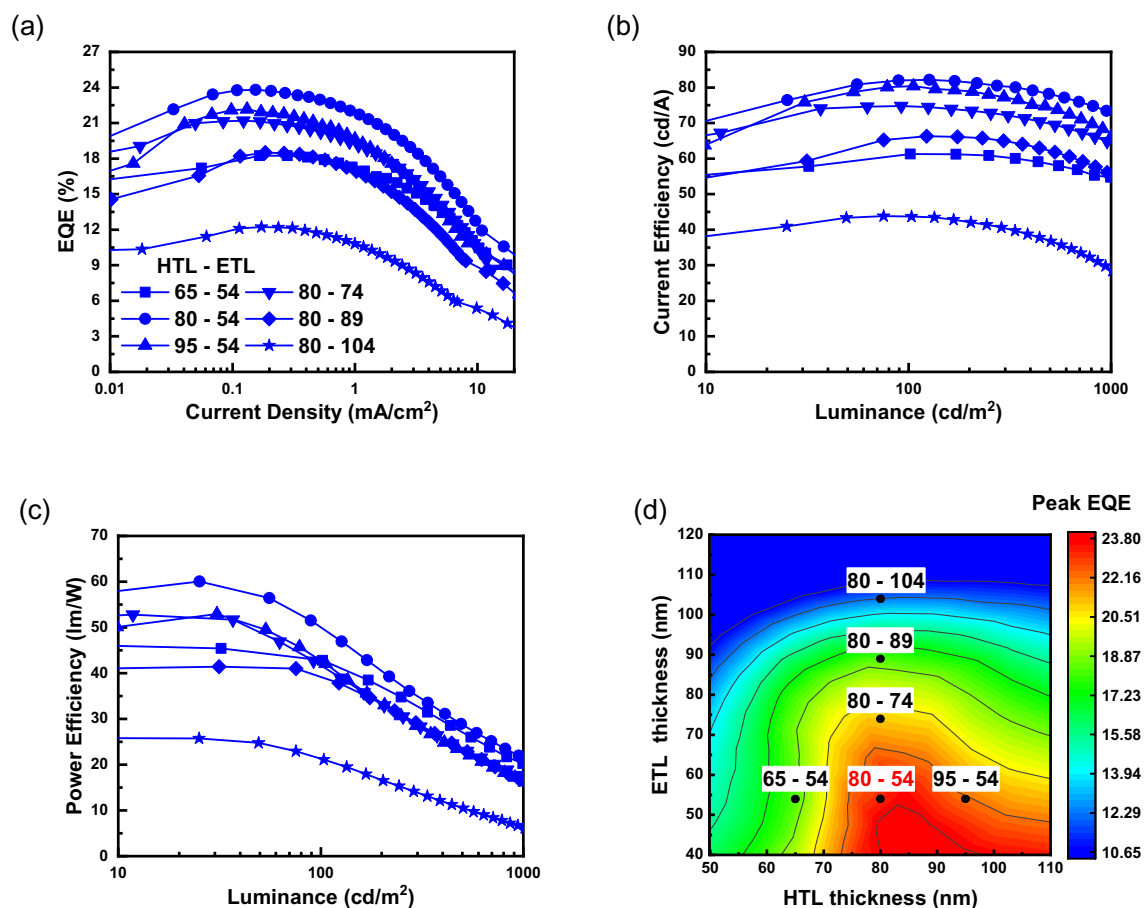


Figure 5. EL characteristics of six representative devices: (a) current density–EQE (J–EQE) characteristics, (b) current efficiency–luminance (CE–L) characteristics, and (c) power efficiency–luminance (PE–L) characteristics. (d) EQE contour plot of all the fabricated OLEDs with various HTL and ETL thickness (the dots are data of the six-representative device).

	ETL thickness			
	54 nm (%)	74 nm (%) ^a	89 nm (%)	104 nm (%)
HTL thickness				
65 nm	18.2 ^b	18.8	16.2	10.7
80 nm ^a	23.8 ^b	21.2 ^b	18.5 ^b	12.2 ^b
95 nm	22.2 ^b	19.7	17.4	12.2

Table 1. Summary of peak EQE for different ETL and HTL thickness. ^aReference thickness calculated using refractive index for constructive interference. ^bDevices presented in Fig. 5a–c.

The decrease in efficiency caused by an increase in ETL thickness could be due to the carrier imbalance. In this structure, this signifies that the mobility of the ETL is much lower than that of the HTL. In addition, as presented in Supporting Information-3, the device is hole-dominant. Therefore, the ETL must be thinner than the HTL. This result suggests that the carrier balance is dominant in this device structure, and that the optical efficiency affected by the internal interference is less effective in here. The peak EQE dependence on the HTL and ETL thickness is summarized and presented in Table 1.

The optical and electrical optimizations of the ultra-thin EML OLEDs were conducted by adjusting the thickness of the dopant, ETL, and HTL. The maximum EQE of the fabricated OLEDs with the ultra-thin Ir(ppy)₃ EML structure was 23.8%, and the device was fabricated without employing a doping process. However, as shown in the graph in Fig. 5a, an EQE roll-off was observed at high current densities. At a current density of 10 mA/cm², the EQE roll-off was ~50% of the peak EQE. Nevertheless, the proposed device achieved 23.8% of maximum EQE, which was the highest EQE, when compared to that of the previously reported ultra-thin OLEDs^{17,19}. The efficiency was relatively higher than that of the conventional doping methods that did not use a novel host or

	Peak EQE (%)	Doping method	Dopant	Note
This work	23.8	Undoped (ultra-thin EML)	Ir(ppy) ₃	0.075 nm thickness of dopant TCTA/TmPyPB interface
¹⁷	20.9	Undoped (ultra-thin EML)	Ir(ppy) ₂ acac	0.1 nm thickness of dopant TCTA/TmPyPB interface
¹⁹	21.1	Undoped (ultra-thin EML)	Ir(ppy) ₂ acac	0.3 nm thickness of dopant TCTA/TmPyPB interface
²⁴	21.2	Conventional	Ir(ppy) ₃	Using novel host Ir(ppy) ₃ , 6 wt% DCzBPI
²⁵	25.5	Conventional	Ir(ppy) ₃	Heavy doping and high mobility ETL ETL: B4PyPPM Ir(ppy) ₃ , 17 wt% doped CBP

Table 2. Summary of peak EQE in this study and in previous works.

transporting layer²⁴ it was also comparable to that of the highest efficiency device²⁵. Table 2 shows a summary of the peak EQE characteristics of the Ir(ppy)₃ devices with highest efficiency.

The OLED structure used in this study did not satisfy the optical path and charge balance requirements, simultaneously, and the EQE roll-off phenomenon occurred; nevertheless, the results demonstrated the highest EQE, when compared to that of other reports^{17,19,24,25}.

The strategy for inserting ultra-thin dopants into high-efficiency OLEDs is simple, and is summarized below.

1. The thickness of ultra-thin dopant with highest efficiency is determined.
2. Using a simple optically optimized structure (transport layer thickness, HTL–ETL), the thickness of the HIL–EIL that can provide the highest efficiency is determined, and the refractive-index difference and mobility are disregarded.
3. The HTL–ETL thickness is finely optimized, considering the refractive-index difference and mobility.

Therefore, using alternative high-mobility ETL materials, low-driving-voltage materials, etc., and applying the wide-emission-zone method utilizing multiple insertions of ultra-thin EMLs can enable the requirements of optical path and charge balance to be satisfied, simultaneously, producing OLEDs with high efficiency and low efficiency roll-off.

Conclusion

In this study, highly efficient phosphorescent OLEDs were fabricated by inserting Ir(ppy)₃ dopants in the form of ultra-thin films, without using conventional doping methods. In order to maximize the IQE of OLEDs with ultra-thin EML structures, the dopant thickness was controlled precisely, and the thicknesses of the injection and charge-transport layers were changed systematically for analysing and characterizing the optical efficiency induced by internal interference and charge-carrier balance. As a result, the proposed device exhibited one of the highest levels of EQE (23.8%), among the observed research results of phosphorescent OLEDs using Ir(ppy)₃ that did not employ any light-extraction technology or other novel layer materials. This exemplary result could be owed to the complex contribution of efficient energy transfer, minimization of exciton dissipation, and optimization of optical internal interference structures and charge balance. This suggests that the OLED devices with ultra-thin EML structures can achieve ultra-high efficiency, comparable to that of the conventional doping technologies. By combining the proposed technology with other technologies, further research and enhancement can be expected, including reduced efficiency roll-off and high power efficiency.

Methods

The OLEDs were fabricated on a commercially purchased indium tin oxide (ITO)-coated STN-LCD glass substrate. The substrates were pre-cleaned through ultrasonication using acetone, methanol, and DI water, in that order. Before thermal evaporation was conducted, the surface of ITO was treated using UV ozone and O₂ plasma, in sequence. The structure of the OLEDs is described as follows. ITO 185 nm in thickness was used as the anode, HAT-CN was used as the HIL, and TAPC and TCTA were used as the HTL. Ir(ppy)₃ was used as the ultra-thin EML, TmPyPB was used as the ETL, LiF was used as the EIL, and Al was used as the cathode. All the organic materials were purchased from Sigma-Aldrich and Lumtec Corp. The vacuum level of the process chamber was maintained at $\sim 3 \times 10^{-7}$ Torr. During the evaporation of all materials, the substrates were rotated at a constant speed of 12 rpm. The organic materials evaporated at a rate of ~ 1 Å/s, and the emitting dopant evaporated at a rate of ~ 0.01 Å/s. LiF evaporated at a rate of ~ 0.1 Å/s, and Al evaporated at a rate of ~ 4 Å/s. The fabricated devices were stored in a glove box, in an Ar atmosphere containing less than 1 ppm of H₂O. A 6-MHz gold-coated quartz crystal microbalance (QCM) and a thin-film deposition controller with a PCI Express interface (IQM-233, INFICON) were used to detect the thickness of the film during the high-vacuum thermal deposition of each thin film. The thickness of the organic materials was measured under an over 98% lifetime of QCM. For precise control of the ultra-thin films, the thickness of each film was calibrated with a thick film of thickness over 500 nm, using a field-emission scanning electron microscope (JSM-6700F, JEOL Co. Ltd) aided by a surface profilometer (Alpha-Step 500, KLA-Tencor). The EL characteristics of the fabricated OLEDs were measured using a spectroradiometer (CS-1000, Konica Minolta Co., Ltd.) and source meter (Keithley-2400, Tektronix) in a dark

box at 25 degrees Celsius (°C) and air atmosphere. The EL efficiency was calculated under the assumption that the OLED was a Lambertian light source.

Received: 26 October 2020; Accepted: 12 March 2021

Published online: 19 April 2021

References

1. Tang, C. W. & VanSlyke, S. A. Organic electroluminescent diodes. *Appl. Phys. Lett.* **51**(12), 913–915 (1987).
2. Tao, J. *et al.* Highly transparent, highly thermally stable nanocellulose/polymer hybrid substrates for flexible OLED devices. *ACS Appl. Mater. Interfaces* **12**(8), 9701–9709 (2020).
3. Yin, D. *et al.* Efficient and mechanically robust stretchable organic light-emitting devices by a laser-programmable buckling process. *Nat. Commun.* **7**, 11573 (2016).
4. Huang, X., Qu, Y., Fan, D., Kim, J. & Forrest, S. R. Ultrathin, lightweight and flexible organic light-emitting devices with a high light outcoupling efficiency. *Org. Electron.* **69**, 297–300 (2019).
5. Eritt, M., May, C., Leo, K., Toerker, M. & Radehaus, C. OLED manufacturing for large area lighting applications. *Thin Solid Films* **518**(11), 3042–3045 (2010).
6. Fan, C. *et al.* Highly efficient, solution-processed orange–red phosphorescent OLEDs by using new iridium phosphor with thieno[3,2-c]pyridine derivative as cyclometalating ligand. *Org. Electron.* **14**(12), 3392–3398 (2013).
7. Chen, J. *et al.* Solution-processable small molecules as efficient universal bipolar host for blue, green and red phosphorescent inverted OLEDs. *J. Mater. Chem.* **22**(11), 5164 (2012).
8. Baldo, M. A. *et al.* Highly efficient phosphorescent emission from organic electroluminescent devices. *Nature* **395**(6698), 151–154 (1998).
9. Uoyama, H., Goushi, K., Shizu, K., Nomura, H. & Adachi, C. Highly efficient organic light-emitting diodes from delayed fluorescence. *Nature* **492**(7428), 234 (2012).
10. Dias, F. B. *et al.* Triplet harvesting with 100% efficiency by way of thermally activated delayed fluorescence in charge transfer OLED emitters. *Adv. Mater.* **25**(27), 3707–3714 (2013).
11. Aydemir, M. *et al.* High efficiency OLEDs based on anthracene derivatives: The impact of electron donating and withdrawing group on the performance of OLED. *Org. Electron.* **30**, 149–157 (2016).
12. Zhang, Q. *et al.* Nearly 100% internal quantum efficiency in undoped electroluminescent devices employing pure organic emitters. *Adv. Mater.* **27**(12), 2096–2100 (2015).
13. Baldo, M. A., Adachi, C. & Forrest, S. R. Transient analysis of organic electrophosphorescence. II. Transient analysis of triplet-triplet annihilation. *Phys. Rev. B.* **62**(16), 10967–10977 (2000).
14. Reineke, S., Walzer, K. & Leo, K. Triplet-exciton quenching in organic phosphorescent light-emitting diodes with Ir-based emitters. *Phys. Rev. B.* **75**(12), 125328 (2007).
15. Mao, H. T. *et al.* Achieving high performances of nondoped OLEDs using carbazole and diphenylphosphoryl-functionalized Ir(III) complexes as active components. *Inorg. Chem.* **56**(16), 9979–9987 (2017).
16. Reineke, S., Rosenow, T. C., Lüssem, B. & Leo, K. Improved high-brightness efficiency of phosphorescent organic LEDs comprising emitter molecules with small permanent dipole moments. *Adv. Mater.* **22**(29), 3189–3193 (2010).
17. Zhao, Y., Chen, Y. & Ma, D. Ultrathin nondoped emissive layers for efficient and simple monochrome and white organic light emitting diodes. *ACS Appl. Mater. Interfaces* **5**(3), 965–971 (2013).
18. Xu, T. *et al.* Wide color-range tunable and low roll-off fluorescent organic light emitting devices based on double undoped ultrathin emitters. *Org. Electron.* **37**, 93–99 (2016).
19. Wu, S., Li, S., Sun, Q., Huang, C. & Fung, M.-K. Highly efficient white organic light-emitting diodes with ultrathin emissive layers and a spacer-free structure. *Sci. Rep.* **6**, 25821 (2016).
20. Xu, T. *et al.* Highly simplified tandem organic light-emitting devices incorporating a green phosphorescence ultrathin emitter within a novel interface exciplex for high efficiency. *ACS Appl. Mater. Interfaces* **9**(12), 10955–10962 (2017).
21. Kawamura, Y. *et al.* 100% phosphorescence quantum efficiency of Ir (III) complexes in organic semiconductor films. *Appl. Phys. Lett.* **86**, 071104 (2005).
22. Baldo, M. A., Lamansky, P. E., Burrows, P. E., Thompson, M. E. & Forrest, S. R. Very high-efficiency green organic light-emitting devices based on electrophosphorescence. *Appl. Phys. Lett.* **75**, 4 (1999).
23. Ye, H. *et al.* Pyridine-containing electron-transport materials for highly efficient blue phosphorescent OLEDs with ultralow operating voltage and reduced efficiency roll-off. *Adv. Funct. Mater.* **24**(21), 3268–3275 (2014).
24. Zhang, X. *et al.* Novel host materials based on phenanthroimidazole derivatives for highly efficient green phosphorescent OLEDs. *J. Photochem. Photobiol. A Chem.* **268**, 37–43 (2013).
25. Sasabe, H. *et al.* Extremely low operating voltage green phosphorescent organic light-emitting devices. *Adv. Funct. Mater.* **23**(44), 5550–5555 (2013).

Acknowledgements

This work was supported by the National Research Foundation of Korea (NRF) Grant funded by the Korean Government (MSIT) (Nos. 2020R1C1C1013567 and 2019R1A2B5B01070286), and Brain Korea 21 Project in 2021. We express our gratitude to the Center for Next Generation Semiconductor Technology at SUNMOON University for their support with the analysis.

Author contributions

S.W.K. conducted the experiments of OLEDs fabrication and analysed the results. D.H.B advised about the result of analysed data. B.-K.J and Y.W.P supervised the project.

Competing interests

The authors declare no competing interests.

Additional information

Supplementary Information The online version contains supplementary material available at <https://doi.org/10.1038/s41598-021-86333-9>.

Correspondence and requests for materials should be addressed to B.-K.J. or Y.W.P.

Reprints and permissions information is available at www.nature.com/reprints.

Publisher's note Springer Nature remains neutral with regard to jurisdictional claims in published maps and institutional affiliations.



Open Access This article is licensed under a Creative Commons Attribution 4.0 International License, which permits use, sharing, adaptation, distribution and reproduction in any medium or format, as long as you give appropriate credit to the original author(s) and the source, provide a link to the Creative Commons licence, and indicate if changes were made. The images or other third party material in this article are included in the article's Creative Commons licence, unless indicated otherwise in a credit line to the material. If material is not included in the article's Creative Commons licence and your intended use is not permitted by statutory regulation or exceeds the permitted use, you will need to obtain permission directly from the copyright holder. To view a copy of this licence, visit <http://creativecommons.org/licenses/by/4.0/>.

© The Author(s) 2021